A New Image Watermarking Method in Wavelet Domain Using Hessenberg and Grey Wolf Optimizer Decomposition

Mohammad Mehdi Piroozmandan

Department of Computer Engineering, Eram Higher Education Institute, Shiraz, Iran.piroozmandan@eram-shiraz.ac.ir

Abstract

Watermark acts as an efficient solution for preventing the unauthorized utilization of digital media. This technique contributes significantly to the protection of property rights through the incorporation of copyright-related information or other identification signs within digital content. This paper proposes a novel robust image watermarking scheme in the wavelet domain based on Grey Wolf Optimizer (GWO) using Hessenberg decomposition. The proposed method consists of three new algorithms. The first new algorithm applies the redistributed invariant discrete wavelet transform (RIDWT) to the host image to obtain an invariant wavelet domain. Following the RIDWT transform, the low-frequency sub-band of wavelet transformed image is segmented into non-overlapping blocks. Subsequently, the most suitable blocks are selected using the sum of visual and edge entropies for the watermark embedding. In this algorithm, the watermark embedding process is performed by Hessenberg decomposition. In the second new algorithm, the watermark extraction process from the watermarked host image is performed using Hessenberg decomposition. Furthermore, the Grey Wolf Optimizer (GWO) is employed in the third proposed algorithm to obtain optimized threshold and compensation parameters. The proposed method in this paper was evaluated using two standard measures, NC and PSNR, and demonstrated significantly better performance than other methods. In addition to its simplicity, this method exhibits strong robustness against image variations and manipulations and substantially improves image quality.

Keywords: Grey Wolf Optimizer, Invariant wavelet transform, Image watermarking, Optimization, Hessenberg decomposition.
.Article history: Received 2025/01/13; Revised 2025/02/29; Accepted 2025/04/24, Article Type: Research paper
© 2025 IAUCTB-IJSEE Science. All rights reserved
https://doi.org/10.82234/ijsee.2025.1196468

1. Introduction

In recent years, with the expansion of the internet and the rapid growth of computer network technology, digital information and content can be distributed at low cost and without loss of quality. Moreover, creating digital content with quality similar to the original using advanced technologies is sometimes easy. This makes it challenging to protect digital content, as a lack of consumer awareness of intellectual property rights can sometimes lead to serious and critical misuse of digital content. Furthermore, images may be intentionally or unintentionally manipulated and altered during transmission through insecure communication channels such as the internet. Since the accuracy of images, including medical images, is sometimes crucial for accurate disease diagnosis, developing effective methods for verifying image authenticity and detecting manipulated areas is one of the challenging and interesting issues for researchers. Digital watermarking refers to embedding information invisibly within digital media such as video, audio, or image to prove ownership or transmit information secretly. Today, digital image watermarking techniques play a significant role in image processing research and applications. They serve as a safeguard for protecting digital image content, copyright, authentication, and ownership verification. Also, when images are shared on the Internet, a major requirement is to ensure copyright protection of one's multimedia, which is where Digital Image Watermarking (DIW) comes into play. Watermarking can embed ownership information within a digital image, allowing for the tracking of its origin and enabling legal action against unauthorized use.In recent years, various methods have been developed for digital image watermarking, which can be categorized into two main domains: spatial and frequency.

Spatial domain watermarking techniques are relatively simple, directly manipulating pixel values in the host image. This simplicity often comes at the cost of robustness against attacks such as compression and noise. While these techniques offer low computational complexity, they are more susceptible to attacks than frequency domain methods. Additionally, the limitations of using spatial domain techniques in watermarking are as follows:

- Weakness against signal processing attacks
- Lack of robustness against geometric attacks
- Limited embedding capacity
- Trade-off between imperceptibility and robustness
- Vulnerability to statistical attacks
- Dependence on the host image
- Lack of post-processing for increased robustness

In frequency domain techniques and methods, watermark images are embedded by modifying the transformed coefficients of the host image. Techniques in the frequency domain analyze images using transformations like the Discrete Fourier Transform (DFT), Discrete Cosine Transform (DCT), and Discrete Wavelet Transform (DWT). These methods generally provide enhanced robustness and adaptability because they extract frequency components from the image. This allows for embedding watermarks in less perceptible image regions, making them more resilient to attacks [24]. Watermarking techniques can be categorized into three main types: robust, fragile, and semi-fragile.

Robust watermarking is designed to withstand unauthorized changes and manipulations, such as embedding additional information, geometric attacks, and image processing. In other words, robust watermarks are embedded to be detected and extracted even after various modifications are applied to the original data. Robust watermarks are typically used to protect copyrights and prove legal ownership. Fragile watermarks are highly susceptible to alterations, and any tampering with the data will result in the total annihilation of the watermark. Fragile watermarks are used to detect tampering and verify data integrity. Semi-fragile watermarking algorithms are robust against noise and minor manipulations, enabling successful watermark extraction. However, extensive structural changes in the data significantly reduce the reliability of watermark retrieval.

The prime objective of a robust watermarking scheme is to preserve the quality of the watermarked image while protecting the watermark when the watermarked image undergoes intentional or unintentional threats. Therefore, a robust watermarking scheme is one in which the watermark stays intact with the content of the host image when it is subjected to different distortions or attacks like rotation, row or column flipping, scaling, and translation.

This article is arranged in sections (2) motivation, (3) Related works, (4) Redistributed invariant discrete wavelet transform (RIDWT), (5) Hessenberg decomposition, (6) GWO, (7) proposed method, (8) experimental results, and section (9) conclusion.

2. Motivation

Soft computing techniques have provided solutions to a wide range of problems, including gray-scale image watermarking.

The proposed watermarking scheme is a novel and robust hybrid system based on Hessenberg decomposition and GWO, which is resistant to various manipulations and attacks while preserving image quality. The novelty of our proposed scheme highlights as follows:

- The proposed scheme applies the redistributed invariant wavelet transform proposed by Li et al. [44] to obtain an invariant wavelet domain.
- The embedding blocks are selected using HVS (sum of visual and edge entropies) for the watermark embedding instead of random selection to obtain the better watermarked image with higher quality and robustness.
- It is clear from the survey of image watermarking literature that the performance of the schemes can be improved by using HD (Hessenberg Decomposition) with the other transforms such as DWT, DCT, and DFT. Therefore, unlike the scheme [45], the proposed scheme applies HD in invariant wavelet transform domain.
- Instead of manually adjusting the threshold and compensation parameters, as in [45], we have obtained their optimized value using GWO.
- It is worth pointing out that GWO that has been successfully implemented for solving complex optimization problems in various fields is being applied for improving the image watermarking scheme for the first time in this paper to the best of authors' knowledge.

3. Related works

In recent years, various methods and techniques in the field of image watermarking based on transforms such as Discrete Cosine Transform (DCT) [1-4], Singular Value Decomposition (SVD) [5-7], Fourier transform [8], Kekre Transform [9], Discrete Wavelet Transform (DWT) [10-12], QR decomposition [13, 14], Arnold Transform, Slantlet and Contourlet transforms [15] have been employed. Recent advancements in AI, leveraging techniques like cellular automata, fuzzy logic, and neural

networks, have significantly enhanced image watermarking. These AI-powered methods enable the design of robust watermarks resistant to various attacks. For instance, a study in [16] combines Integer Wavelet Transform (IWT) and Singular Value Decomposition (SVD) to create a multi-scale and secure watermarking scheme. In [17], a blind optical color watermark scheme is proposed with single-pixel imaging (SPI), redistributed invariant lifting wavelet transform (RILWT) and singular value decomposition (SVD), in which the watermark is first encrypted by the SPI and then embedded into host image with SVD in redistributed invariant wavelet domain. In [18], an optimized color image watermarking algorithm with stationary wavelet transforms and singular value decomposition has been proposed in this work. The algorithm uses two watermarks to address copyright protection issues and tamper localization. A grey-scale image watermark is embedded in the transform domain of the green plane of the cover image to address the issue of copyright protection. In [19], an image watermarking technique is proposed. In the proposed method, hybrid signals are used as watermarks. Hybrid means using images as well as an audio signal as watermarks. This can certainly increase the robustness of the proposed technique as in case of very rigorous attacks, at least one watermark can be survived, ensuring the valid owner of the signal being sent. The watermarks are inserted in different levels of the host image using the entire energy distribution of the host image. The energy of the watermarks is divided to embed different parts of the energy in various levels of the host signal. For this, discrete wavelet transform (DWT) and singular value decomposition (SVD) are used. In [20], a blind dual watermarking scheme for color images is proposed by embedding an invisible robust watermark to protect copyright, as well as a fragile watermark is embedded for image authentication. For the purpose of copyright protection, the robust watermark is embedded into the blue channel of RGB color space based on DWT, HVS and SVD domains using a specialized PSO optimization to balance the trade-off between robustness and imperceptibility. In addition, the robust watermarking capacity in SVD is doubled by inserting two robust watermark bits into each selected blocks and the robust watermark can be extracted blindly. For the purpose of authentication, a fragile watermark is embedded into all channels of RGB color space using a new way to manipulate the diagonal singular values. The authenticity of a suspected image can be verified in the absence of original watermark and host images. The combination of robust and fragile watermarking in the proposed scheme provides a suitable mechanism to protect valuable and original color images. In [21], a robust and imperceptible watermarking scheme is presented by combining canny edge detection and contourlet transform with singular value decomposition to enhance the invisibility and robustness of the watermarking algorithm. The contourlet transform first decomposes the host image. Then, the low-frequency sub-band obtained by the contourlet transform is partitioned into 4×4 non-overlapping blocks, and the singular value decomposition is carried out for the specific blocks selected by the canny edge detection. Finally, the watermark is embedded into the coefficient of matrix U. The embedded watermark could be recovered blindly in the watermark extraction stage. The robustness and the imperceptibility are efficiently guaranteed with an optimal threshold k selected by the least-square curve fitting. This study [22] proposes a watermarking method based on discrete wavelet transform and singular value decomposition for copyright protection. This method decomposes the target image into sub-bands using the discrete wavelet transform. Then, the low-frequency sub-band is divided into non-overlapping blocks. These blocks are transformed into U, S, and V matrices using singular value decomposition.

Many fragile watermarking methods have been proposed for image authentication and digital image integrity protection. However, these methods still suffer from unsatisfactory quality in watermarked images and low accuracy in tampering detection. In the method proposed by Thai-Son Nguyen [23], a new fragile watermarking scheme for image authentication is proposed based on the combination of discrete wavelet transform, discrete cosine transform, and singular value decomposition. A modulation in the quantization index process extracts coefficients in the transforms and embeds the authentication code. Furthermore, the Gram-Schmidt process is used to ensure the correctness of the extracted authentication code.

In [25], deep learning is used to identify the appropriate location for embedding the mark.in this method, a deep network mask region-based CNN was developed and trained on the Common Objects in context dataset. Although the experimental results demonstrated good transparency and robustness of the marked data, the security of the watermark needs to be further investigated. In [26] presented a robust watermarking scheme using a cycle variational autoencoder. The network learned to embed and extract 1-bit mark images, improving their visual quality. However, its watermark capacity was low, limiting the use of the method for practical applications. In [27] 2022, Ge et al. proposed a document image watermarking scheme using an encoder-decoder network. The scheme used the noise layer and watermark expansion approach to improve resilience against attacks. However, the scheme was embedded-strength dependent and performed poorly against JPEG attacks.

In 2020, Zhong et al. [28] designed a hiding scheme based on the convolutional network. Two different networks were used to embed and extract the watermark. Additionally, a fully connected invariant network was used to learn the noise variations in the watermarked image to improve robustness. However, the network's end-to-end training led to information loss. In 2021, Ding et al. [29] proposed a watermarking scheme using a deep neural network. Initially, Up-sampling was applied on the cover and mark images using the transpose convolutional network. After that, a blender network blended the watermark and cover images. Subsequently, a sampler was used to obtain a marked image. The extractor network was composed of a convolutional block to extract the watermark. Though this scheme achieved high invisibility, it did not always produce good resilience against attacks such as JPEG, median and low-pass filtering and rotation attacks.

This paper proposes a robust image watermarking scheme using three new algorithms in the invariant wavelet domain.

In the proposed method, a redistributed invariant discrete wavelet transform (RIDWT) is first applied to the host image to obtain a domain of stationary wavelet coefficients. Then, the low-frequency sub-band of this transformed image is divided into non-overlapping blocks. Using the human visual system (HVS) model blocks less sensitive to changes (i.e., lower visual and edge entropy) are selected for watermark embedding. This selection is because changes in these blocks are less likely to be detected by the human observer. In this algorithm, the watermark embedding process is performed by Hessenberg decomposition. In the second new algorithm, the watermark extraction process from the watermarked host image is performed using Hessenberg decomposition. Furthermore, the third proposed algorithm, the grey wolf optimizer (GWO), is employed to obtain optimized threshold and compensation parameters.

4. Redistributed invariant discrete wavelet transform (RIDWT)

Discrete Wavelet Transform (DWT) is one of the most widely used mathematical transformations in processing, especially signal and image processing. Although most existing watermarking schemes based on DWT have survived typical image processing attacks, there is still scope for improvement for attacks like geometric distortions such as multiples of rotation and image flipping. A wavelet domain image watermarking system that is invariant to image flipping and multiples of 90◦ rotation was proposed by [31] to overcome this challenge. The method presented in this article by Li et al. is called Redistributed Invariant Discrete Wavelet Transform (RIDWT). Redistributed invariant discrete wavelet transform (RIDWT) is based on the fact that a multiple of rotation and image flipping change only the locations of the pixels in the image, but their intensities are left unchanged. According to it, the image's pixels' locations are redistributed; then, the Haar wavelet transform and some normalized procedures are performed, and the invariant wavelet domain is obtained.

In this method, the original image (I) with size M × N is divided into four equal-sized sub-images of size2×2. The mean intensity of pixels in each sub-image (m_{ij}) is stored in a matrix named M as follows:

$$M = \begin{bmatrix} m_{11} & m_{12} \\ m_{21} & m_{22} \end{bmatrix} \tag{1}$$

Then, matrix M is normalized to form matrix NM according to equation (2):

$$\begin{aligned} NM &= \begin{bmatrix} NM_{11} & NM_{12} \\ NM_{21} & NM_{22} \end{bmatrix} \\ &= \begin{bmatrix} m_{11}+m_{12}+m_{21}+m_{22} & m_{11}-m_{12}+m_{21}-m_{22} \\ m_{11}-m_{21}+m_{12}-m_{22} & m_{11}-m_{12}+m_{22}-m_{21} \end{bmatrix} \end{aligned} \tag{2}$$

The sign matrix is constructed using equation (3):

$$SG = \begin{bmatrix} SG_{11} & SG_{12} \\ SG_{21} & SG_{22} \end{bmatrix}, SG_{ij} \begin{cases} 1 & if\ NM_{ij} > 0 \\ -1 & if\ NM_{ij} < 0 \end{cases} \tag{3}$$

Redistribute the original image (I) using the distribution relation given in (4) to obtain the redistributed image (RI).

$$\begin{cases} RI(2i-1,2j-1) = I(i,j) & 1 \le i \le \frac{M}{2}, 1 \le j \le \frac{N}{2} \\ RI(2i-1,2j-1) = I\left(i, 3\frac{N}{2} - j + 1\right) & 1 \le i \le \frac{M}{2}, \frac{N}{2} \le j \le N \\ RI(2i-M,2j-1) = I\left(3\frac{M}{2} - i + 1, j\right) & \frac{M}{2} \le i \le M, 1 \le j \le \frac{N}{2} \\ RI(2i-M,2j-N) = I\left(3\frac{M}{2} - i + 1, 3\frac{N}{2} - j + 1\right) & \frac{M}{2} \le i \le A, \frac{N}{2} \le j \le N \end{cases} \tag{4}$$

Then, apply the one level Haar wavelet transform to the image RI that decompose it into four sub-bands, namely LL, HL, LH and HH such that RI $\xrightarrow{DWT} \begin{pmatrix} LL & HL \\ LH & HH \end{pmatrix}$ and multiply the sub-band of the transformed image by the Sign matrix, as given below and denote the resulted matrix as:

$$\mathrm{Z} = \begin{pmatrix} \mathrm{Z}_{11} & \mathrm{Z}_{12} \\ \mathrm{Z}_{21} & \mathrm{Z}_{22} \end{pmatrix} = \begin{pmatrix} \mathrm{SG}_{11} \times \mathrm{LL} & \mathrm{SG}_{12} \times \mathrm{HL} \\ \mathrm{SG}_{21} \times \mathrm{LH} & \mathrm{SG}_{22} \times \mathrm{HH} \end{pmatrix} \tag{5}$$

The matrix Z is just the invariant wavelet domain if $|NM_{21}| < |NM_{12}|$, where the term |*| is the absolute value operator. Otherwise, swap Z_{12} with Z_{21} , and transpose each sub-band of Z to get a refreshed matrix Z, that is $Z = \begin{pmatrix} Z_{11}^T & Z_{12}^T \\ Z_{21}^T & Z_{22}^T \end{pmatrix}$ where Z_{ij}^T denotes the transpose matrix of Z_{ij}. The final matrix Z is the invariant wavelet domain; that is invariant to multiples of 90°rotation and row or column flipping.

5. Hessenberg decomposition

In 1996, Golub and his colleague introduced the Hessenberg decomposition [36]. This decomposition factorizes a general matrix A using orthogonal transformations, as shown in equation (6).

$$A = QHQ^T \ (6) \quad (6)$$

In equation (6), Q is an orthogonal matrix, and H is an upper Hessenberg matrix. Also, if $i > j + 1$, then $h_{i,j} = 0$. The Hessenberg decomposition is usually calculated using Householder matrices, and the Householder matrix P is calculated using equation (7).

$$p = (I_n - 2uu^T)/u^T u \ (7) \quad (7)$$

In equation (7), I_n and u represent the identity matrix of size $N \times N$ and a non-zero vector in R^n, respectively.

There are *n*-2 steps in the overall procedure when A is of size $n \times n$. Therefore, Hessenberg decomposition is computed as follows:

$$H = (p_1 p_2 \dots p_{n-3} p_{n-2})^T A (p_1 p_2 \dots p_{n-3} p_{n-2}) (8) \quad (8)$$

$$H = Q^T AQ \quad (9)$$

$$A = QHQ^T \quad (10)$$

In equations (9) and (10), Q is obtained from the following equation:

$$Q = p_1 p_2 \dots p_{n-3} p_{n-2} \quad (11)$$

6. Grey Wolf Optimization Technique

The grey wolf optimization algorithm known as GWO is introduced in [43]. GWO algorithm is a successful swarm intelligence algorithm inspired by the hunting behavior and social leadership of grey wolves. In this meta-heuristic method, four grey wolf models, alpha(α), beta, (β) delta(δ), and omega(ω), simulate the leadership hierarchy. Also, this algorithm uses the three main stages of hunting, namely, searching for prey, surrounding the prey, and attacking the prey. Like most meta-heuristic algorithms, the GWO algorithm starts with a random population. In the GWO algorithm, the mathematical model of the social hierarchy of wolves considers the best solution to be alpha wolf, and the second and third solutions are considered beta and delta. The rest of the candidate solutions are assumed to be Omega. In the grey wolf optimization algorithm, hunting (optimization) is guided by alpha, beta, and delta wolves; omega wolves follow these three wolves. The mathematical model of the surrounding behavior of grey wolves that surround the prey during hunting is in the form of the following relationships:

$$D = \left|\vec{C}.\overrightarrow{X_P}(t) - \vec{X}(t)\right| \quad (12)$$

$$\vec{X}(t+1) = \left|\overrightarrow{X_p}(t) - \vec{A}.\vec{D}\right| \quad (13)$$

(t) is the current iteration, (A) and (C) are coefficient vectors, $\overrightarrow{X_p}(t)$ is the position vector of prey, and $\vec{X}(t)$ is the position vector of the grey wolf. The vectors $\vec{A}$ and $\vec{D}$ are calculated as follows:

$$\vec{A} = 2\vec{a}.\vec{r_1} - \vec{a} \quad (14)$$

$$\vec{C} = 2.\vec{r_2} \quad (15)$$

The vectors $\vec{r_1}$ and $\vec{r_2}$ are random vectors in the interval [0,1], and the components decrease linearly with the increase in the number of repetitions from 2 to 0. Grey wolves can detect the location of prey and surround them. The alpha wolf usually leads the hunt. Beta and delta wolves may participate in hunting at times. In order to mathematically simulate the hunting behavior of grey wolves, it is assumed in the GWO algorithm that alpha (the best solutions), beta, and delta have good information about the potential of the prey location. Therefore, we save the three best solutions obtained so far and force the rest of the search agents to update their positions based on the positions of the best agents. For this purpose, the following relationships are suggested.

$$\overrightarrow{D_\alpha} = \left|\overrightarrow{C_1}.\overrightarrow{X_\alpha} - \vec{X}\right|, \overrightarrow{D_\beta} = \left|\overrightarrow{C_2}.\overrightarrow{X_B} - \vec{X}\right|, \overrightarrow{D_\delta} = \left|\overrightarrow{C_3}.\overrightarrow{X_\delta} - \vec{X}\right| \quad (16)$$

$$\overrightarrow{X_1} = \overrightarrow{X_\alpha} - A_1.\left(\overrightarrow{D_\alpha}\right), \overrightarrow{X_2} = \overrightarrow{X_\beta} - A_2.\left(\overrightarrow{D_\beta}\right), \overrightarrow{X_3} = \overrightarrow{X_\delta} - A_3.\left(\overrightarrow{D_\delta}\right) \quad (17)$$

$$\overrightarrow{X_1}(t+1) = \frac{\overrightarrow{X_1} + \overrightarrow{X_2} + \overrightarrow{X_3}}{3} \quad (18)$$

7. Proposed method

This section is dedicated to explaining the proposed method as follows:

A) Watermark embedding

The primary objective of Algorithm 1 is to embed additional information (a watermark) into a base image (host image). Specifically, a 32×32 pixel binary watermark image, denoted as W, is embedded within a 512×512 pixel grayscale host image, denoted as I. The detailed steps involved in executing this algorithm are as follows:

Algorithm 1:

1) The host image I is divided into non-overlapping 8×8 blocks, and then we go to step 2.
2) By utilizing the characteristics of the Human Visual System (HVS), we calculate the visual

and edge entropies of the created non-overlapping blocks (4096 created blocks) and obtain the sum of each, and then we go to step 3.

3) We arrange the sum of the visual and edge entropies of each non-overlapping block in ascending order, and then we go to step 4.
4) We select the first 1024 blocks for watermark embedding. The row and column of the selected blocks are stored, and then we go to step 5.
5) Using the stored row and column information, we retrieve the 1024 blocks and apply the RIDWT transform to them (The result of this transformation is four sub-bands namedZ_{11},Z_{12}, Z_{21} and Z_{22}) , and then we go to step 6.
6) We select Z_{11} and apply the Hessenberg decomposition to it, obtaining two components, $Q_{i,j}$ and $H_{i,j}$, and then we go to step 7.
7) To embed the watermark, we calculate the following equation for each matrix Q within the selected blocks (μ is calculated for the selected blocks), and then go to step 8.

$$\mu = \frac{|Q_{2,3}| + |Q_{2,4}|}{2} \quad (19)$$

8) If w=1 (w is the binary watermark bit), then as long as $|Q_{2,3} - Q_{2,4}| > T$ and $Q_{2,3} \geq Q_{2,4}$ are not equal, the elements $Q_{2,3}$and $Q_{2,4}$ are calculated as (20),(21) Else if w=0, then as long as $|Q_{2,3} - Q_{2,4}| > T$ and $Q_{2,3} < Q_{2,4}$ are not equal, the elements $Q_{2,3}$and $Q_{2,4}$ are calculated as (22),(23). The results are stored in the matrix$Q_{i,j}^{w}$, and then we go to step 9.

$$Q_{2,3} = \mu + \frac{T}{2} \quad (20)$$

$$Q_{2,4} = \mu - \frac{T}{2} \quad (21)$$

$$Q_{2,3} = \mu - \frac{T}{2} \quad (22)$$

$$Q_{2,4} = \mu + \frac{T}{2} \quad (23)$$

9) The inverse of the Hessenberg decomposition is obtained for each watermarked block according to the following equation. The inverse of the Redistributed Invariant Discrete Wavelet Transform (RIDWT) is applied to the sub-bandsz_{11}^{w}, Z_{21}, Z_{12}, and Z_{22} to obtain the watermarked host image I_W.

$$z_{11}^{w} = Q_{ij}^{w} . H_{ij} . Q_{ij}^{w^T} \quad (24)$$

B) Watermark extraction

Watermark extraction is performed using the following algorithm:

Algorithm 2:

1) The watermarked host image (I_W) is divided into non-overlapping blocks of size 8x8 pixels, and then we go to step 2.
2) The blocks previously identified for watermark embedding are utilized to locate the corresponding blocks containing the embedded watermark information. By applying the inverse RIDWT to these blocks, the sub-bands Z'_{11},Z'_{12} , Z'_{21} and Z'_{22} are extracted, and then we go to step 3.
3) Hessenberg decomposition is applied to each 4x4 block Z'_{11} to obtain the two components, $Q1_{i,j}$ and $H1_{i,j}$,and then we go to step 4.
4) The watermark is extracted by examining elements $Q1_{2,3}$ and $Q1_{2,4}$ of matrix $Q1_{i,j}$ as follows:

$$W_{i,j} = \begin{cases} 1 & if\ Q1_{2,3} \geq Q1_{2,4} \\ 0 & otherwise \end{cases} \quad (25)$$

C) Grey wolf optimizer (GWO) algorithm in finding optimal parameters

In watermarking techniques, striking a balance between two key properties, robustness and imperceptibility, is paramount. Robustness refers to the watermark's ability to maintain its integrity after various attacks, such as compression, noise addition, cropping, and rotation. On the other hand, imperceptibility refers to the degree to which the watermark is imperceptible in the original image. One of the primary challenges in watermarking is the trade-off between these two properties. Generally, increasing robustness comes at the expense of decreased imperceptibility and vice versa. The threshold in watermarking, a crucial parameter, significantly influences this balance. Increasing the threshold enhances the watermark's robustness but simultaneously degrades image quality and reduces imperceptibility. Conversely, a lower threshold favors imperceptibility but renders the watermarked image more vulnerable to attacks.To improve this trade-off, various techniques can be employed. For instance, combining spatial-domain and transform-domain watermarking methods can simultaneously enhance robustness and imperceptibility. Additionally, utilizing optimization algorithms to fine-tune watermarking method parameters can help achieve the optimal balance between these two properties.

In the proposed method (Algorithm 3), the Grey Wolf Optimizer (GWO) is employed to balance robustness and imperceptibility and automatically determine the optimal threshold value

based on the watermarked image. Algorithm 3 is as follows:

Algorithm 3:

1) Initialize the population size and number of cycles (iterations) and to start the process we have to generate the starting values of wolves by using Eq.(26). W , $lower_b$, and $upper_b$ are the initial values of wolves, lower bound, and upper bound, respectively. Also, rand is the random function in between 0 and 1 and lower and upper bound shows the range of the parameters used in the equation which we have to optimize. Initial values are assigned to the variables a, B, and C.

$$W = lower_b + rand \times (upper_b - lower_b) \quad (26)$$

$$a = 2 \times (1 - \frac{iteration}{maxiteration}) \quad (27)$$

$$A = 2 \times a \times rand - a \quad (28)$$

$$C = 2 \times rand \quad (29)$$

$$Min\ F = |PSNR - PSNR_T| + (1 + \frac{1}{n}\sum_{i=1}^{n} NC_i) \quad (30)$$

$$PSNR(I, I_W) = 10log_{10}\left(\frac{(I_{max})^2}{\frac{1}{n \times n}\sum_{i=1}^{n}\sum_{j=1}^{n}(I_{i,j} - I_W)^2}\right) \quad (31)$$

$$NC(W, W^*) = \frac{\sum_{i=1}^{n}\sum_{j=1}^{n} W_{i,j} \oplus W^*_{i,j}}{n \times n} \quad (32)$$

2) Find the fitness of the initial solution.In equation (30), 'n' defines the number of attacks that are permissible within the established procedure. Furthermore, NC_i denotes the normalized correlation of the extracted watermark (W^*)corresponding to the ith attack, while $PSNR_T$ signifies the target PSNR value.In equations (31) and (32), I,I_W, W, and W^*represent the original host image, the watermarked image, the original watermark image, and the extracted watermark image, respectively.Also, in equation (31) $I_{max}$is the maximum possible intensity value of the image I, for an 8-bit per pixel representation $I_{max}$is 255. In equation (32) $\oplus$ denotes the exclusive –OR (XOR) operation and n is the height or width of the square image.
3) Calculate the fitness of each search solution
   - $S_\alpha = the\ best\ search\ solution$
   - $S_\beta = the\ second\ best\ search\ solution$
   - $S_\delta = the\ third\ best\ search\ solution$
4) Update the position of the current search solution

$$\vec{S}(t+1) = \frac{\vec{S_1} + \vec{S_2} + \vec{S_3}}{3} \quad (33)$$

5) Calculate the fitness of the new search solution
6) Store the fitness solution so far attained Iteration=iteration +1. The algorithm stops when the optimal solution is found.

D) Experimental results

The different results obtained from the proposed method based on Algorithms 1, 2 and 3 presented in this paper are discussed in this section. For experimental simulation, MATLAB (2023a) environment was utilized in this study with 8 GB RAM, i9 3.0 GHz processor, and 3 TB memory. Figure 1 illustrates example images used in this study: Barbara, airplane, cameraman, baboon, parrot, boat, hills, Lena, man, Monarch, along with the watermark image (a binary logo with dimensions 32×32 pixels). The proposed method was evaluated on a dataset of 611 standard images, each with 512×512 or 768×768 pixels dimensions.

In this paper, the proposed method's performance is evaluated in comparison to other methods, and the accuracy of the extracted watermark is assessed. To this end, Peak Signal-to-Noise Ratio (PSNR) and Normalized Cross-Correlation (NC) are employed as evaluation measures.

$$PSNR = 10log_{10}\frac{MN \times [Max(I(m,n))]^2}{\sum_{m=1}^{M}\sum_{n=1}^{N}[I(m,n) - I_W(m,n)]^2} \quad (34)$$

Where I is the original image and I_W is a watermarked image with the same size M × N. In addition, to measure the extracted watermark's accuracy, the Normalized Cross (NC) is used to compare the quality of the extracted watermark and original watermark image. The Normalized Cross (NC) is defined as:

$$NC = \frac{\sum_{m=1}^{M}\sum_{n=1}^{N} w(m,n).w^*(m,n)}{\sqrt{\sum_{m=1}^{M}\sum_{n=1}^{N}(w(m,n)^2 \cdot \sum_{m=1}^{M}\sum_{n=1}^{N}(w^*(m,n)^2}} \quad (35)$$

Where M and N are the size of the original watermark image w and extracted watermark imagew^*.The performance of the method proposed in this article has been evaluated using different methods and schemes, Methods such as M. Ali [37] ،E.H. Elshazly[38] ,which we will call FWT ، Md.A Hussian [39] ، H.K Singh [40] ، D. Liu [41] ، Q. Wei [42] ، X. Zhong [43]. In order to validate the robustness of the proposed method, several image manipulation attacks are applied to degrade the quality of the watermarked image I_W, which are briefly described in Table 1 with their indexes.

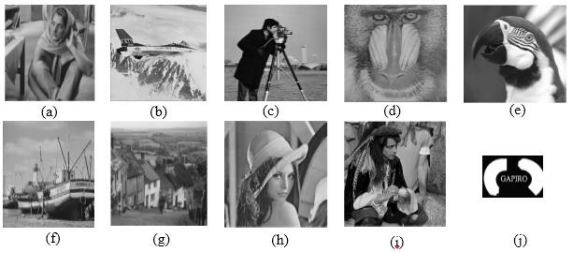

Fig. 1. An example of (a-j) test images Barbara, Airplane, Cameraman, Baboon, Parrot, Boat, Hills, Lena and Man from 611 test images and (j) watermark image.

Table.1.
Description of the attacks used for the robustness analysis

Index	*Attack's description*
1	No attack applied
2	Median filtering with window size 2×2
3	Rescaling 512→256→512
4	Gamma correction with gamma value 0.2
5	Anticlockwise rotation by 90°
6	Circular cropping with 256 radius and centered at the center of the image
7	Histogram equalization
8	Gaussian noise addition with mean zero and standard deviation 0.15
9	JPEG compression with quality factor 75
10	Salt and pepper noise with noise density 0.2
11	Deleted 91 rows and 91 columns from random locations
12	Gaussian low pass filter with window size 9 × 9
13	Sharpening
14	Contrast adjustment (enhanced 40%)
15	Flipping of rows
16	Flipping of columns

An effective watermarking scheme should maintain image quality without noticeable degradation. Ideally, the watermarked image should be visually indistinguishable from the original. Furthermore, a successful watermarking method must be imperceptible to the human eye, and its performance should be evaluated through objective and subjective evaluations. Imperceptibility, a crucial aspect of watermarking, is inherently linked to the characteristics of the Human Visual System (HVS). To ensure invisibility, the embedded watermark must be imperceptible to the human eye. One objective evaluation Measure employed in this study is Peak Signal-to-Noise Ratio (PSNR), as summarized in Table 2. This table presents the PSNR values achieved by the proposed method and its comparison with other state-of-the-art techniques.

〖PSNR〗_T within the table represents the target PSNR, serving as a performance threshold. The results demonstrate that the proposed method outperforms the existing approaches, while the methods of X. Zhong [43], E.H. Elshazly[38], and M. Ali [37] exhibit relatively poorer performance. The histograms of the original and watermarked images were analyzed to evaluate the subjective impact of watermarking. Figure 2 presents the histogram results for the original images (Barbara, Baboon, and Lena) and their corresponding watermarked versions. The visual similarity between the histograms of the original and watermarked images in Figure 2 provides strong evidence for the imperceptibility of the proposed watermarking method. Tables 3 and 4 present the extracted watermark quality, evaluated using the NC value. The numerical results demonstrate a positive correlation between the similarity between the extracted and original watermarks and the corresponding NC value.

E) Robustness against attacks

This section evaluates the robustness of the proposed scheme against the attacks that are given in Table 1. The quality of the extracted watermark is determined by calculating the NC value using (35) and the corresponding results are tabulated in Tables 3 and 4. A higher NC value indicates that the extracted watermark is more similar to the original watermark. Table 3 shows the results of the watermark extracted from the images that have not been subjected to any distortion attacks. From this table, it is clear that the methods D. Liu [41], H.K Singh [40], Q. Wei [42], X. Zhong [43] and the proposed method have extracted the watermark. Notably, the methods of E.H. Elshazly [38] and M. Ali [37] exhibit lower performance compared to others and demonstrate reduced robustness against attacks. Table 4 presents the average NC values achieved by the proposed method and seven other techniques across thirty-eight test images. These images were subjected to various attacks, as outlined in Table 2. The results demonstrate that the proposed method outperforms the other techniques. Notably, the methods of E.H. Elshazly [38], X. Zhong [43], and M. Ali [37] exhibited lower performance compared to the others.Figure 3 illustrates a sample of the attacks applied to the watermarked 'baboon' image.Figure 4 presents the visual quality of the recovered watermark, demonstrating that the methods proposed by X. Zhong [43], M. Ali [37], and E.H. Elshazly [38] exhibit lower performance compared to others. While the methods of H.K. Singh [40], D. Liu [41], and Md. A Hussian [39] achieves comparable performance; they also outperform the aforementioned methods, particularly in the presence of Gaussian noise and flipping attacks. Furthermore, figure 4 demonstrates that the proposed method significantly outperforms other techniques in watermark extraction. Figure 4 presents the visual quality of the recovered watermark, demonstrating that the methods proposed by X. Zhong [43], M. Ali [37], and E.H. Elshazly [38] exhibit lower performance compared to others. While the methods of H.K. Singh [40], D. Liu [41], and Md. A Hussian [39] achieves comparable performance; they also outperform the

aforementioned methods, particularly in the presence of Gaussian noise and flipping attacks. Furthermore, figure 4 demonstrates that the proposed method significantly outperforms other techniques in watermark extraction.

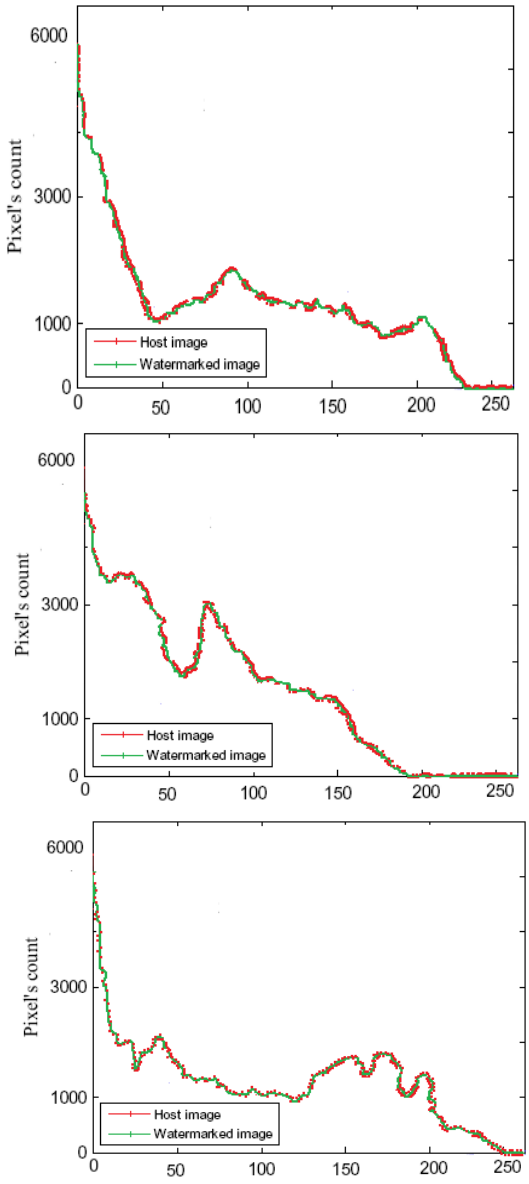

Fig. 2. Transparency or imperceptibility illustration through histograms taking images (a) Barbara, (b) Baboon and (c) Lena.

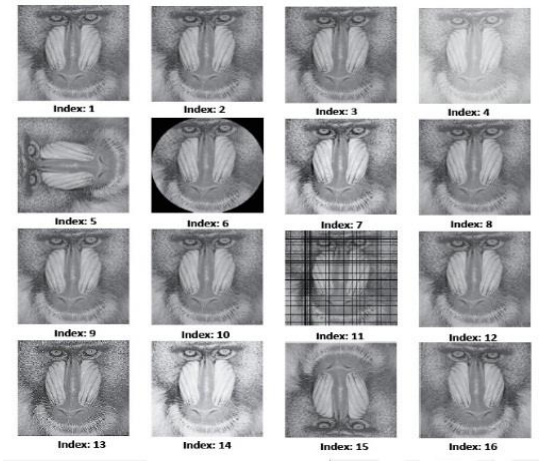

Fig. 3. Visual representation of the attacks applied to the watermarked images

8. Conclusion

This paper proposes an effective method for image watermarking in the wavelet domain based on three new algorithms. One advantage of the proposed method is that embedding blocks are selected based on the Human Visual System (HVS) using the sum of visual entropy and edge information. This feature ensures that the generated watermarks have higher quality and robustness. In other words, the watermarks are more visible and better preserved against changes made to the original image. Furthermore, in the proposed method, instead of manually adjusting the parameters, we employed a novel algorithm (Algorithm 3) based on grey wolf optimizer (GWO) to find the optimal settings. This significantly enhances the accuracy and quality of the results. In this paper, the results of various methods are compared both visually and quantitatively. Evaluations based on the NC (Normalized Correlation) and PSNR (Peak Signal to Noise Ratio) measures demonstrate that the proposed method outperforms existing approaches. One of the important advantages of our proposed method is its high robustness against image attacks. Our method has exhibited superior resilience to fifteen different types of image manipulations. Moreover, the evaluation of the proposed method on color images presents an intriguing research avenue for future work, which the authors intend to explore.

Table.2.
PSNR between watermarked and original images

Image	*M. Ali [37]*	*E.H. Elshazly[38]*	*Md.A Hussian [39]*	*H.K Singh [40]*	*D. Liu [41]*	*Q. Wei [42]*	*X. Zhong [43]*	$PSNR_T$	*Proposed method*
Lena	38.11	37.45	41.07	42.42	41.18	40.71	39.01	43	43.19
Zelda	47.78	46.88	50.22	51.63	50.37	49.02	48.22	52	52.12
Houses	38.01	37.11	41.78	42.28	41.88	40.88	39.11	43	43.18
Man	29.11	28.44	41.18	42.48	41.91	40.77	30.01	43	43.28
Babbon	40.08	39.77	43.11	44.77	43.28	42.44	41.22	45	45.88
Couple	43.22	42.54	46.71	47.88	46.78	45.11	44.01	48	48.11
Sailboat	41.77	40.22	44.78	46.22	45.11	43.74	42.47	47	47.08
Kiel	40.54	39.52	45.77	47.18	46.88	42.81	41.11	48	48.22

Table.3.
Comparison of the schemes in terms of NC value of extracted watermark obtained from the watermarked images without any distortion attacks

Image	*M. Ali [37]*	*E.H. Elshazly[38]*	*Md.A Hussian [39]*	*H.K Singh [40]*	*D. Liu [41]*	*Q. Wei [42]*	*X. Zhong [43]*	*Proposed method*
Lena	1.00	1.00	41.07	1.00	1.00	1.00	1.00	1.00
Zelda	0.9988	0.9979	50.22	1.00	1.00	1.00	1.00	1.00
Houses	0.9874	0.9861	41.78	0.9921	1.00	0.9902	0.9881	1.00
Man	0.9794	0.9744	41.18	0.9988	0.9901	0.9812	0.9801	1.00
Babbon	0.9873	0.9832	43.11	1.00	0.9981	0.9919	0.9883	1.00
Couple	0.9801	0.9784	46.71	0.9902	0.9882	0.9839	0.9811	0.9938
Sailboat	0.9788	0.9729	44.78	0.9922	0.9903	0.9822	0.9804	0.9989
Kiel	0.9981	0.9919	45.77	1.00	1.00	1.00	1.00	1.00

Table.4.
Comparison of the methods in terms of NC value obtained by taking over the thirty-eight host images corresponding to the different distortion attacks.

Index	*M. Ali [37]*	*E.H. Elshazly[38]*	*Md.A Hussian [39]*	*H.K Singh [40]*	*D. Liu [41]*	*Q. Wei [42]*	*X. Zhong [43]*	*Proposed method*
1	0.9519	0.9498	0.9897	0.9938	0.9909	0.9778	0.9681	0.9993
2	0.8829	0.8749	0.9111	0.9201	0.9191	0.9001	0.8919	0.9219
3	0.8998	0.9019	0.9251	0.9304	0.9294	0.9115	0.9059	0.9322
4	0.9539	0.9449	0.9892	0.9968	0.9909	0.9739	0.9693	0.9996
5	0.8798	0.8601	0.8898	0.9001	0.8902	0.8719	0.8691	0.9021
6	0.9589	0.9459	0.9809	0.9902	0.9888	0.9798	0.9688	0. 9992
7	0.9493	0.9438	0.9795	0.9821	0.9802	0.9651	0.9509	0.9891
8	0.9219	0.9198	0.9401	0.9509	0.9419	0.9319	0.9398	0.9598
9	0.9011	0.9002	0.9389	0.9421	0.9401	0.9291	0.9101	0.9442
10	0.8921	0.8898	0.9411	0.9509	0.9491	0.9411	0.9019	0.9533
11	0.8829	0.8798	0.9819	0.9908	0.9899	0.9701	0.8959	0.9989
12	0.9201	0.9119	0.9594	0.9623	0.9604	0.9449	0.9398	0.9643
13	0.9819	0.9794	0.9902	0.9951	0.9919	0.9819	0.9709	0.9994
14	0.9508	0.9498	0.9818	0.9884	0.9851	0.9721	0.9619	0.9881
15	0.9449	0.9401	0.9839	0.9901	0.9893	0.9708	0.9529	0.9994
16	0.9309	0.9298	0.9894	0.9921	0.9902	0.9718	0.9491	0.9991
Average	0.9252	0.9201	0.9607	0.9672	0.9642	0.9496	0.9341	0.9700

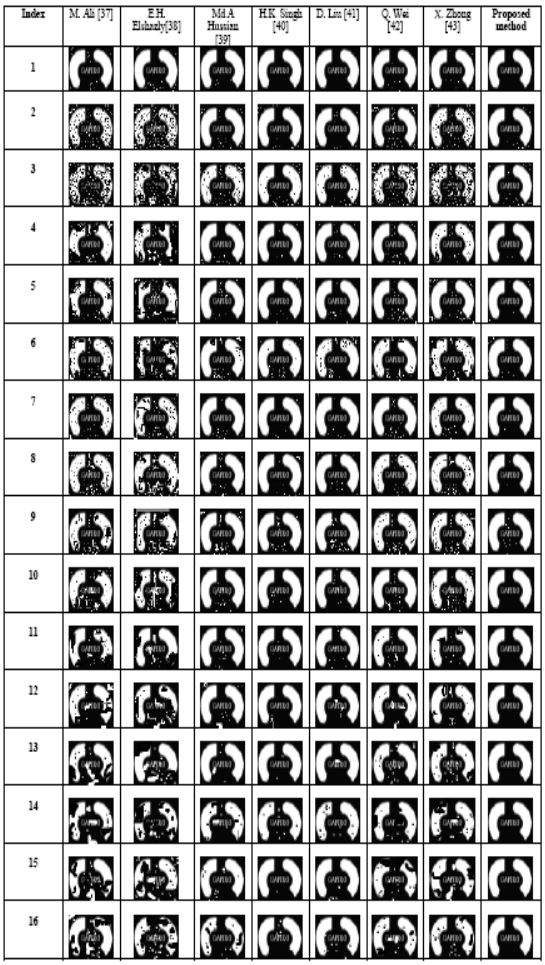

Fig. 4. Extracted Watermarks from the 'Baboon' Image using Various Methods

References

[1] S. P. Mohanty , B. K. Bhargava, "Invisible watermarking based on creation and robust insertion-extraction of image adaptive watermarks," ACM Transactions on Multimedia Computing Communications and Applications, 5(2), pp. 1-24,2008.

[2] S. Fazli , M. Moeinib, , "Robust image watermarking method based on DWT, DCT, and SVD using a new technique for correction of main geometric attacks," Optik, 127, pp. 964-972,2016.

[3] S. A. Parah, J. A. Sheikh, N. A. Loan and G. M. Bhat, "Robust and blind watermarking technique in DCT domain using inter-block coefficient differencing," Digital Signal Processing, 53, pp. 11-24, 2016.

[4] A. Benoraira, K. Benmahammed and N. Boucenna, , "Blind image watermarking technique based on differential embedding in DWT and DCT domains," EURASIP Journal on Advances in Signal Processing, 2015, pp. 1-11,2015.

[5] E. Najafi and K. Loukhaoukha, "Hybrid secure and robust image watermarking scheme based on SVD and sharp frequency localized contourlet transform," Journal of Information Security and Applications, 44, pp. 144-156,2019.

[6] I. A. Ansari and M. Pant, "Multipurpose image watermarking in the domain of DWT based on SVD and ABC," Pattern Recognition Letters, 94, pp. 228-236, 2017.

[7] J. L. D. Shivani and R. K. Senapati, , "False-positive-free, robust and blind watermarking scheme based on Shuffled SVD and RDWT," Journal of Advanced Research in Dynamical & Control Systems, 10(06)-Special Issue, pp. 1971-1981,2018.

[8] Hu, Y., and Z. Wang, "A geometric distortion resilient image watermark algorithm based on DWT-DFT," Journal of Software, 6 (9), pp. 1805-1812, 2011.

[9] H. B. Kekre, T. Sarode and S. Natu, "Robust watermarking for color images using SVD with row/column wavelet transform in low and mid-frequency spectrum of host," Advances in Image and Video Processing, 2 (6), 2014.

[10] X. L. Liu, C. C. Lin and S. M. Yuan, "Blind dual watermarking for color images' authentication and copyright protection," IEEE Transactions on Circuits and Systems for video technology, (28) 5, pp. 1047-1055, 2018.

[11] T. Huynh-The, C. H. Hua, N. A. Tu, T. Hur, J. Bang, D. Kim, M. B. Amin, B. H. Kang, H. Seung and S. Lee, "Selective bit embedding scheme for robust blind color image watermarking," Information Sciences, 426, pp. 1-18, 2018.

[12] S. T. Chen, H. N. Huang, W. M. Kung and C. Y. Hsu, "Optimization-based image watermarking with integrated Quantization embedding in the wavelet domain," Multimedia Tools and Applications, 75(10), pp. 5493-5511, 2016.

[13] Q. Su, Y. Niu, G. Wang, S. Jia and J. Yue, "Color image blind watermarking scheme based on QR decomposition," Signal Processing, 94, pp. 219-235, 2014.

[14] L. Laur, P. Rasti, M. Agoyi and G. Anbarjafari, "A robust color image watermarking scheme using entropy and QR decomposition," Radioengineering, 24(4), pp. 1025-1031, 2015.

[15] M. Mardanpour and M. A. Z. Chahooki, "Robust transparent image watermarking with Shearlet transform and bidiagonal singular value decomposition," International Journal of Electronics and Communications, 70, pp. 790-798, 2016.

[16] Luo, Y., et al., A multi-scale image watermarking based on integer wavelet transform and singular value decomposition. Expert Systems with Applications, 168: p. 114272, 2021.

[17] Qu, G., et al., Optical color watermarking based on single-pixel imaging and singular value decomposition in invariant wavelet domain. Optics and Lasers in Engineering, 137: p. 106376, 2021.

[18] Sivananthamaitrey, P. and P.R. Kumar," Optimal Dual Watermarking of Color Images with SWT and SVD Through Genetic Algorithm", Circuits, Systems, and Signal Processing, 41(1): p. 224-248, 2022.

[19] Singha, A. and M.A. Ullah, "An image watermarking technique using hybrid signals as watermarks", Multimedia Systems, 27(1): p. 89-109, 2021.

[20] Ahmadi, S.B.B., et al., "An intelligent and blind dual color image watermarking for authentication and copyright protection", Applied Intelligence, 51(3): p. 1701-1732, 2021.

[21] Gong, L.-H., et al., "Robust and imperceptible watermarking scheme based on Canny edge detection and SVD in the contourlet domain", Multimedia Tools and Applications, 80(1): p. 439-461, 2021.

[22] Altay, Ş.Y. and G. Ulutaş, "Self-adaptive step firefly algorithm based robust watermarking method in DWT-SVD domain", Multimedia Tools and Applications, 80(15): p. 23457-23484, 2021.

[23] [23] T.S Nguyen," Fragile watermarking for image authentication based on DWT-SVD-DCT techniques". Multimedia Tools and Applications,80(16): p. 25107-25119, 2021.

[24] Kumar C, Singh AK, Kumar P ," A recent survey on image watermarking techniques and its application in e-governance", Multimedia Tools Appl, 77:3597–3622, 2018.

[25] Bagheri M, Mohrekesh M, Karimi N, Samavi S, Shirani S, Khadivi P ," Image watermarking with region of interest determination using deep neural networks", In 2020 19th IEEE International Conference on Machine Learning and Applications (ICMLA). IEEE, pp 1067–1072, 2020.

[26] Wei Q, Wang H, Zhang G," A robust image watermarking approach using cycle variational Autoencoder". Secur Commun Netw, 2020.

[27] Ge S, Xia Z, Fei J, Sun X, Weng J , "A robust document image watermarking scheme using deep neural network", arXiv preprint arXiv:2202.13067,2022.

[28] Zhong X, Huang PC, Mastorakis S, Shih FY ,"An automated and robust image watermarking scheme based on deep neural networks" IEEE Trans Multimedia 23:1951–1961, 2022.

[29] Ding W, Ming Y, Cao Z, Lin CT ," A generalized deep neural network approach for digital watermarking analysis", IEEE Trans Emerg Top Comput Intell 6(3):613–627, 2021.

[30] M. Ali, C.W. Ahn, "An optimized watermarking technique based on self-adaptive DE in DWT–SVD transform domain", Signal Process. 545–556, 2014.

[31] L. Li, H.-H. Xu, C.-C. Chang, Y.-Y. Ma, "A novel image watermarking in redistributed invariant wavelet domain", J. Syst. Softw. 923–929, 2011.

[32] R. Liu, T. Tan, "An SVD-based watermarking scheme for protecting rightful ownership", IEEE Trans. Multimed. 121–128,2 003.

[33] M.M.Piroozmandan, F.Farokhi, K.Kangarloo, M.Jahanshahi," Removing High Density Impulse Noise via a Novel Two Phase Method Using Fuzzy Cellular Automata", International Journal of Smart Electrical Engineering, 177 – 186, 2021.

[34] M.M.Piroozmandan, F.Farokhi, K.Kangarloo, M.Jahanshahi," Removing the impulse noise from images based on fuzzy cellular automata by using a two-phase innovative method", Optik –International Journal for Light and Electron Optics , 168-713, 2022. https://doi.org/10.1016/j.ijleo.2022.168713.

[35] Mohammad Mehdi Piroozmandan , Fardad Farokhi , Mohammad Ali Piroozmandan, "International Journal of Smart Electrical Engineering ", 147 – 155, 2024.

[36] G.H Golub, C,F,V Loan,"Matrix computations", Johns Hopkins University Press, Baltimore, 1996.

[37] M. Ali , Ch.W Ahn , M. Pant , P. Siarry , "An image watermarking scheme in wavelet domain with optimized compensation of singular value decomposition via artificial bee colony", Information Sciences, 2015, http://dx.doi.org/10.1016/j.ins.2014.12.042.

[38] E.H. Elshazly, O.S. Faragallah, A.M. Abbas, M.A. Ashour, E.-S.M. El-Rabaie, H. Kazemian, et al, "Robust and secure fractional wavelet image watermarking", Signal, Image Video Process. 2014, http://dxdoi.org/10.1007/s11760-014-0684-x.

[39] Md.A Hussian, P. bora, "Novel Watermarking Technique Using Encryption Steganography", Chaotic Logistic Map and Multiple Embedding, Procedia Computer Science,2020. https://doi.org/10.1016/j.procs.2020.04.227.

[40] H.K Singh , A. Kumar Singh, "Digital image watermarking using deep learning", Multimedia Tools and Applications,2024, https://doi.org/10.1007/s11042-023-15750-x.

[41] D. Liu, D. Liu, B. Wang, P. Zheng, "Hybrid domain digital watermarking scheme based on improved differential evolution algorithm and singular value block embedding", IET Image Processing,(2023),https:// 10.1049/ipr2.12814.

[42] Q. Wei, H. Wang, G. Zhang ," A robust image watermarking approach using cycle variational autoencoder". Secur Commun Netw, 2020.

[43] X. Zhong, PC. Huang, S. Mastorakis, FY. Shih, "An automated and robust image watermarking scheme based on deep neural networks", IEEE Trans Multimedia, 2020.

[44] L. Li, H.-H. Xu, C.-C. Chang, Y.-Y. Ma, A novel image watermarking in redistributed invariant wavelet domain, J. Syst. Softw. 84 (2011) 923–929.

[45] M.-Q. Fan, H.-X. Wang, S.-K. Li, Restudy on SVD-based watermarking scheme, Appl. Math. Comput. 203 (2008) 926–930.